

Current-time behaviour for copper electrodeposition.

I. Theoretical analysis based on a surface diffusion model

Y. OGATA*, K. YAMAKAWA, S. YOSHIZAWA

Department of Industrial Chemistry, Kyoto University, Kyoto, Japan

Received 16 October 1981

The form of the current-time transients for copper electrodeposition from copper sulphate solutions have been calculated based on a surface diffusion model. The transient was greatly affected by whether the ad-species diffusing across the surface was ad-atom Cu^0 or ad-ion Cu^+ , and by the surface coverage by the ad-species. The results imply that it is possible to experimentally test the applicability of the surface diffusion model to copper electrodeposition, to identify the ad-species (Cu^0 or Cu^+), to estimate the surface coverage and to calculate the parameters related to surface diffusion, D/l^2 and i_0/c_0 .

1. Introduction

A surface diffusion model has been considered to be one of the most promising models for explaining the mechanism of the electrodeposition of metals. An analysis of potentiostatic experiments has been given by Fleischmann *et al.* [1-3] and Damjanovic and Bockris [4]. The current-time response deduced from the analysis has been demonstrated graphically by Damjanovic and Bockris [4] and Harrison [5]. However, the experimental study of the surface diffusion phenomenon is difficult despite theoretical progress.

In the present study, the analysis of the current-time response based on the surface diffusion model is repeated and the results are applied to the case of copper electrodeposition in acidic copper sulphate solutions. The purpose of the present study is to prepare the way for the experimental examination of the surface diffusion model which will be presented in the successive paper.

2. Theory

2.1. Mathematical treatment of the surface diffusion model

The surface diffusion model has been presented elsewhere [6, 7] and both one [1, 2, 4] and two-dimensional [3] analyses have been given. Here a one-dimensional treatment is presented.

The concentration of the ad-species must reach an equilibrium value, c_0 , over the electrode before a potential is applied. After applying a potential, a concentration gradient is produced due to the consumption at steps of the ad-species and a delay in the transport of the ad-species by surface diffusion. There is a zero concentration gradient at the midpoints of the steps. The situation is shown in Fig. 1. The diffusion equations, and the initial and boundary conditions are as follows, with the coverage of the ad-species taken into account as suggested by Bockris and Kita [8]:

$$\frac{\partial c}{\partial t} = D \frac{\partial^2 c}{\partial x^2} + \frac{i_0}{zF} \frac{1-\theta}{1-\theta_0} \exp\left(-\frac{\alpha_c F}{RT} \eta\right) - \frac{i_0}{zF} \frac{\theta}{\theta_0} \exp\left(\frac{\alpha_a F}{RT} \eta\right) \quad (1)$$

$$\frac{\partial c}{\partial t} = D \frac{\partial^2 c}{\partial x^2} + k_1 - k_2 c. \quad (2)$$

* Present address: Department of Synthetic Chemistry, Nagoya Institute of Technology, Gokiso-cho, Showa-ku, Nagoya 466, Japan.

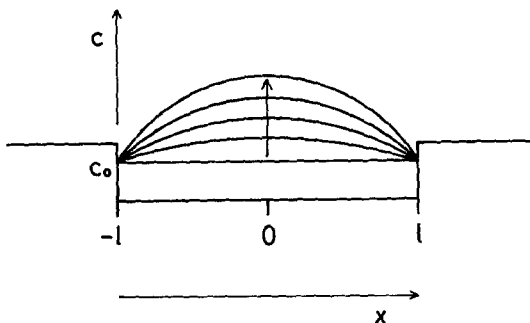


Fig. 1. Concentration profile of ad-species. c_0 : Equilibrium surface coverage of ad-species; $2l$: Distance of steps.

Initial and boundary conditions,

$$t = 0, \quad -l \leq x \leq l; \quad c = c_0 \quad (3)$$

$$t > 0, \quad x = \pm l; \quad c = c_0 \quad (4)$$

$$x = 0; \quad \frac{\partial c}{\partial x} = 0 \quad (5)$$

where,

$$k_1 = \frac{i_0}{zF} \frac{1}{1 - \theta_0} \exp\left(-\frac{\alpha_c F}{RT}\right) \quad (6)$$

$$k_2 = \frac{i_0}{zFN_0} \left[\frac{1}{1 - \theta_0} \exp\left(-\frac{\alpha_c F}{RT} \eta\right) + \frac{1}{\theta_0} \exp\left(\frac{\alpha_a F}{RT} \eta\right) \right] \quad (7)$$

where N_0 is the concentration of sites at which the ad-species can adsorb (g-atom cm^{-2}), θ is the coverage of the ad-species and θ_0 is the equilibrium coverage of the ad-species. The other symbols have their normal meanings. Transformation by introducing $U = c/c_0$, $X = x/l$, $T = Dt/l^2$, $N_1 = l^2 k_1/Dc_0$ and $N_2 = l^2 k_2/D$ in Equations 1 to 5 gives Equations 8 to 10:

$$\frac{\partial U}{\partial T} = \frac{\partial^2 U}{\partial X^2} + N_1 - N_2 U, \quad (8)$$

initial and boundary conditions

$$T = 0; \quad -1 \leq X \leq 1; \quad U = 1 \quad (9)$$

$$T > 0; \quad X = \pm 1; \quad U = 1 \quad (10)$$

$$X = 0; \quad \frac{\partial U}{\partial X} = 0. \quad (11)$$

The solution of this differential equation is [9]

$$U = \frac{N_1}{N_2} - \frac{(N_1/N_2) - 1}{\cosh N_2^{1/2}} \cosh(N_2^{1/2} X) - \sum_{n=0}^{\infty} \frac{(-1)^n 4(N_1 - N_2)}{(2n+1)\pi \left[N_2 + \frac{(2n+1)^2 \pi^2}{4} \right]} \cos \frac{(2n+1)\pi X}{2} \exp\left\{-\left[N_2 + \frac{(2n+1)^2 \pi^2}{4} \right] T\right\}. \quad (12)$$

The result is essentially the same as that obtained by Fleischmann and Thirsk [1] and Damjanovic and Bockris [4].

2.2. Current-time profiles

The deposition and dissolution of copper in acidic copper sulphate are considered to proceed according

to Equations 13 and 14 in which the rate determining step is Equation 13 as Mattson and Bockris [10] have proposed.



The mechanism implies that two different ad-species may be possible, i.e. ad-atom Cu^0 or ad-ion Cu^+ .

The dimensionless current defined as Equation 15 is given by Equation 16.

$$J = \frac{l^2}{Dc_0zF} i \quad (15)$$

$$J = \int_0^1 (N_1 - N_2 U) dX. \quad (16)$$

If the ad-species is Cu^0 , then Cu^{2+} is reduced to Cu^0 and the ad-atom diffuses on a plane. Then, the ad-atom arriving at a step is incorporated into the lattice of the copper metal. The dimensionless current for this situation is

$$J = \frac{N_1 - N_2}{N_2^{1/2}} \tanh N_2^{1/2} + \sum_{n=0}^{\infty} \frac{8(N_1 - N_2)N_2}{(2n+1)^2\pi^2 \left[N_2 + \frac{(2n+1)^2\pi^2}{4} \right]} \exp \left\{ - \left[N_2 + \frac{(2n+1)^2\pi^2}{4} \right] T \right\}. \quad (17)$$

On the other hand, if the ad-species is Cu^+ , the Cu^{2+} is reduced in a one-electron step according to Equation 13 and the ad-ion Cu^+ produced diffuses along a step. Then, the ad-ion is reduced to atomic copper according to Equation 14 and is incorporated into the lattice of the copper substrate. The difference between the two cases is that the contribution of the current at the steps must be considered in the latter instance. Only Fleishmann *et al.* [11] have taken this into consideration. The treatment just before the incorporation of the ad-species at the steps is similar to the case of ad-atom Cu^0 . However, it must be noted that the values of the electrochemical parameters are different from those in the case of ad-atom Cu^0 .

The current at the steps is given by Equation 18 provided the incorporation rate of the ad-ion is sufficiently fast.

$$i = -\frac{zFD}{l} \left(\frac{\partial c}{\partial x} \right)_{x=l} \quad (18)$$

With the transformation to a dimensionless current, Equation 18 becomes Equation 19 and the result is given by Equation 20.

$$J_s = - \left(\frac{\partial U}{\partial X} \right)_{X=1} \quad (19)$$

$$= \frac{N_1 - N_2}{N_2^{1/2}} \tanh N_2^{1/2} - \sum_{n=0}^{\infty} \frac{2(N_1 - N_2)}{\left[N_2 + \frac{(2n+1)^2\pi^2}{4} \right]} \exp \left\{ - \left[N_2 + \frac{(2n+1)^2\pi^2}{4} \right] T \right\}. \quad (20)$$

As a result, the current in this situation becomes the sum of Equations 17 and 20

$$J = \frac{2(N_1 - N_2)}{N_2^{1/2}} \tanh N_2^{1/2} + \sum_{n=0}^{\infty} \frac{8(N_1 - N_2) \left[N_2 - \frac{(2n+1)^2\pi^2}{4} \right]}{(2n+1)^2\pi^2 \left[N_2 + \frac{(2n+1)^2\pi^2}{4} \right]} \exp \left\{ - \left[N_2 + \frac{(2n+1)^2\pi^2}{4} \right] T \right\}. \quad (21)$$

2.3. Current-time transients at OFF

When the overpotential is returned to zero after the steady-state has been attained at the applied potential (we call this situation OFF, whereas the normal applied potential situation is ON), the initial condition is different from that at ON and is given by the steady-state term in Equation 12. The differential equation and conditions are

$$\frac{\partial U}{\partial T} = \frac{\partial^2 U}{\partial X^2} + N_3(1 - U) \quad (22)$$

where

$$N_3 = \frac{i_0 l^2}{zFDc_0}, \quad (23)$$

initial and boundary condition,

$$T = 0, \quad -1 \leq X \leq 1; \quad U = \frac{N_1}{N_2} - \frac{(N_1/N_2) - 1}{\cosh N_2^{1/2}} \cosh(N_2^{1/2} X) \quad (24)$$

$$T > 0; \quad X = \pm 1; \quad U = 1 \quad (25)$$

$$X = 0; \quad \frac{\partial U}{\partial X} = 0. \quad (26)$$

The solution becomes [9]

$$U = 1 + \sum_{n=0}^{\infty} \frac{(-1)^n 4(N_1 - N_2)}{(2n+1)\pi \left[N_2 + \frac{(2n+1)^2 \pi^2}{4} \right]} \cos \frac{(2n+1)\pi X}{2} \exp \left\{ - \left[N_3 + \frac{(2n+1)^2 \pi^2}{4} \right] T \right\}. \quad (27)$$

Current-time responses have to be calculated for the two cases as in the preceding sections. When the ad-atom is Cu^0 , the dimensionless current is given by Equation 29.

$$J = \int_0^1 N_3(1 - U) dX \quad (28)$$

$$= \sum_{n=0}^{\infty} \frac{8N_3(N_2 - N_1)}{(2n+1)^2 \pi^2 \left[N_2 + \frac{(2n+1)^2 \pi^2}{4} \right]} \exp \left\{ - \left[N_3 + \frac{(2n+1)^2 \pi^2}{4} \right] T \right\} \quad (29)$$

When the ad-ion is Cu^+ , the contribution of the current at the steps must be considered as in ON. The contribution is

$$J_s = - \left(\frac{\partial U}{\partial X} \right)_{X=1} \quad (30)$$

$$= \sum_{n=0}^{\infty} \frac{2(N_1 - N_2)}{(2n+1)^2 \pi^2 \left[N_2 + \frac{(2n+1)^2 \pi^2}{4} \right]} \exp \left\{ - \left[N_3 + \frac{(2n+1)^2 \pi^2}{4} \right] T \right\}. \quad (31)$$

The total current is given by the sum of Equations 29 and 31, where the signs are opposite, positive and negative, respectively, according to the oxidation and reduction of the Cu^+ ad-ion

$$J = \sum_{n=0}^{\infty} \frac{8(N_2 - N_1) \left[N_3 - \frac{(2n+1)^2 \pi^2}{4} \right]}{(2n+1)^2 \pi^2 \left[N_2 + \frac{(2n+1)^2 \pi^2}{4} \right]} \exp \left\{ - \left[N_3 + \frac{(2n+1)^2 \pi^2}{4} \right] T \right\}. \quad (32)$$

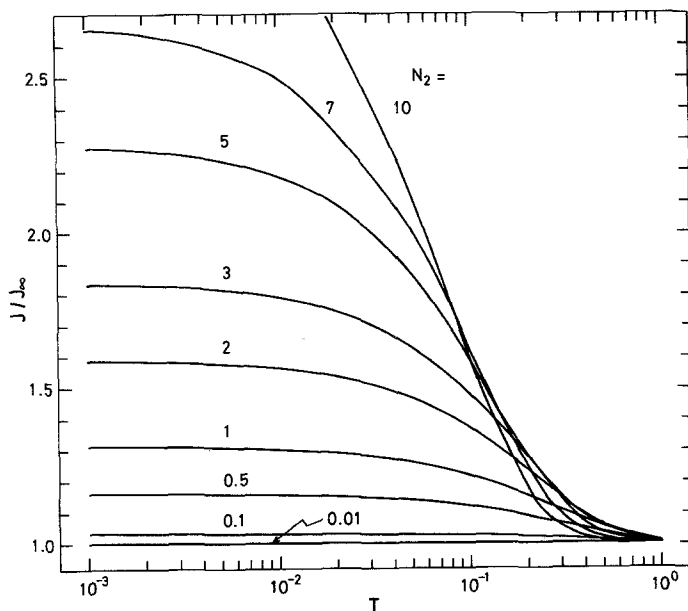


Fig. 2. The relationship between J/J_∞ and time at various N_2 values when the ad-species is the ad-atom Cu^0 .

3. Discussion

Dimensionless current is given by Equation 17 or 21. Calculating J/J_∞ values simplifies Equations 17 and 21, i.e. for ad-atom Cu^0

$$\frac{J}{J_\infty} = \frac{i}{i_\infty} = 1 + \frac{2N_2^{3/2}}{\tanh N_2^{1/2}} \sum_{n=0}^{\infty} \frac{\exp\left\{-\left[N_2 + \frac{(2n+1)^2\pi^2}{4}\right]T\right\}}{(2n+1)^2\pi^2 \left[N_2 + \frac{(2n+1)^2\pi^2}{4}\right]}, \quad (33)$$

and for ad-ion Cu^+

$$\frac{J}{J_\infty} = \frac{i}{i_\infty} = 1 + \frac{N_2^{1/2}}{\tanh N_2^{1/2}} \sum_{n=0}^{\infty} \frac{\left[N_2 - \frac{(2n+1)^2\pi^2}{4}\right] \exp\left\{-\left[N_2 + \frac{(2n+1)^2\pi^2}{4}\right]T\right\}}{(2n+1)^2\pi^2 \left[N_2 + \frac{(2n+1)^2\pi^2}{4}\right]}. \quad (34)$$

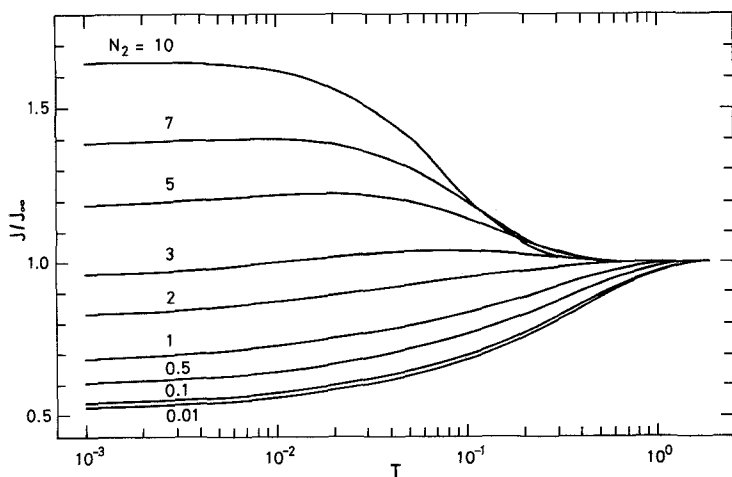


Fig. 3. The relationship between J/J_∞ and time at various N_2 values when the ad-species is the ad-ion Cu^+ .

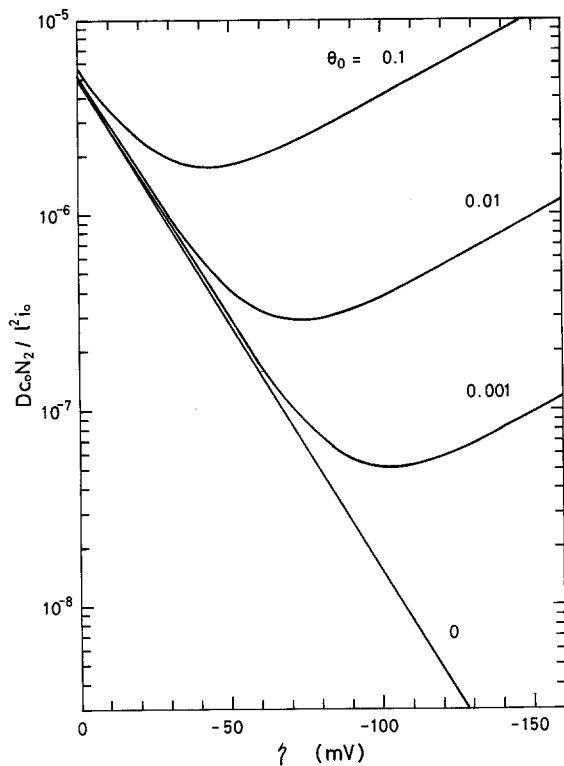


Fig. 4. $Dc_0 N_2 / i^2 i_0$ with varying θ_0 as a function of overpotential in the case of ad-atom Cu^0 .

As seen in Equations 33 and 34, J/J_∞ can be expressed as a function with only one variable, N_2 . In addition, J/J_∞ is directly related to i/i_∞ which is obtained by experiment.

J/J_∞ curves calculated with various N_2 values are shown in Figs. 2 and 3. With an ad-atom intermediate, all curves decrease with time and a major decrease occurs in the two decades preceding the steady-state condition. The extent of the variation in J/J_∞ values increases with increasing N_2 and the curves quickly approach steady-state values at large N_2 . This behaviour implies that the contribution of

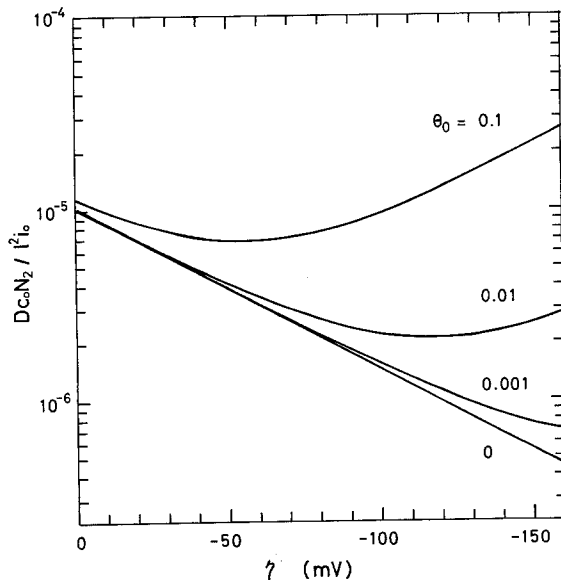


Fig. 5. $Dc_0 N_2 / i^2 i_0$ with varying θ_0 as a function of overpotential in the case of ad-ion Cu^+ .

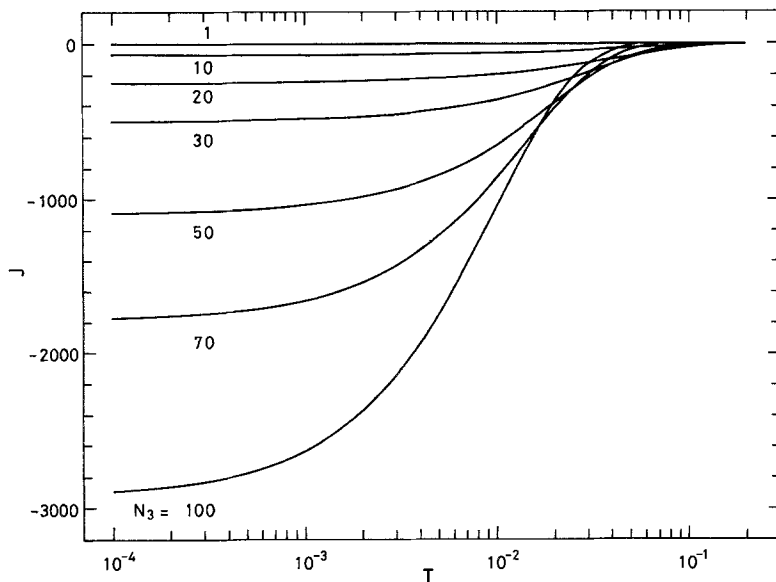


Fig. 6. The relationship between J and time at OFF in the case of ad-atom Cu^0 , $\eta = -50$ mV, $\theta_0 = 0$.

surface diffusion diminishes with decreasing N_2 and the contribution to J/J_∞ with time cannot be found clearly at values of N_2 less than 0.01. On the other hand, with the ad-ion Cu^+ , a different behaviour can be seen at small N_2 values. With N_2 less than 2, J/J_∞ increases with time. J/J_∞ has a maximum at one or two decades before it attains a steady-state value for N_2 values between 3 and 7. Larger N_2 values lead to a J/J_∞ curve shape similar to that of the ad-atom Cu^0 .

The above treatment implies that it is possible to estimate experimentally the parameters involved in surface diffusion. By plotting the experimental curve of i/i_∞ against $\log t$, and the theoretical curves of J/J_∞ against $\log T$, and finding the best fit to the theoretical curves, it is possible to obtain D/l^2 from the abscissa and $l^2 i_0/Dc_0$ from the N_2 value. Moreover, $l^2 i_0/Dc_0$ leads to i_0/c_0 since D/l^2 is already known.

The parameter which determines a J/J_∞ transient is N_2 as seen clearly in Equations 33 and 34. The dependence of N_2 on overpotential is shown in Figs. 4 and 5 for ad-atom Cu^0 and ad-ion Cu^+ , respectively, where $Dc_0 N_2/l^2 i_0$ is chosen as the ordinate instead of N_2 since parameters related to surface diffusion are unknown. $Dc_0 N_2/l^2 i_0$ is given by

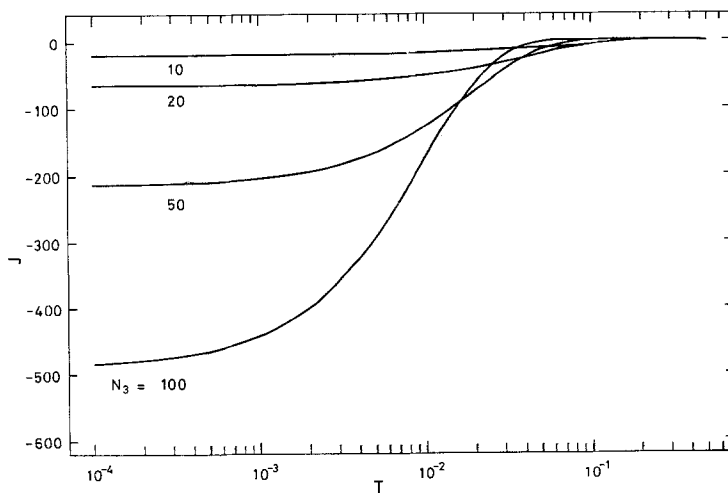


Fig. 7. The relationship between J and time at OFF in the case of ad-ion Cu^+ , $\eta = -50$ mV, $\theta_0 = 0$.

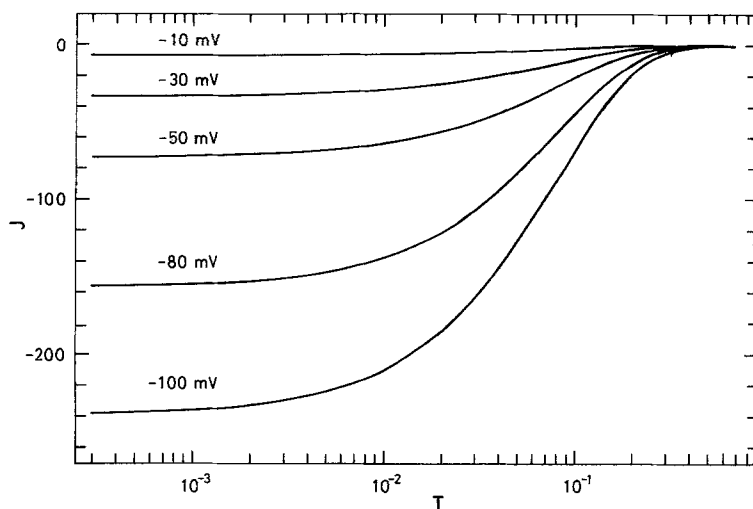


Fig. 8. The relationship between J and time with varying η at OFF in the case of ad-atom Cu^0 , $\theta_0 = 0$, $N_3 = 10$.

$$\frac{Dc_0}{l^2 i_0} N_2 = \frac{1}{zF} \left[\frac{\theta_0}{1 - \theta_0} \exp\left(-\frac{\alpha_c F}{RT} \eta\right) + \exp\left(\frac{\alpha_a F}{RT} \eta\right) \right] \quad (35)$$

In the absence of a surface coverage of ad-species, N_2 decreases linearly with increasing logarithm of the cathodic overpotential. Surface coverage affects N_2 very much and as a result, the variation of J/J_∞ with time. The variation of N_2 with overpotential in the presence of surface coverage has a minimum. This means that the J/J_∞ (or i/i_∞)-time relationship is the same at low overpotential as at a certain higher overpotential since N_2 has the same value at two different overpotentials.

In the case of OFF, some of the ad-species existing on planes returns to solution according to the reaction: $\text{Cu}^0 \rightarrow \text{Cu}^{2+} + 2e$ or $\text{Cu}^+ \rightarrow \text{Cu}^{2+} + e$; the remainder is incorporated into the lattice at steps on the electrode according to the reaction $\text{Cu}^0 \rightarrow \text{Cu}_{\text{lattice}}$ or $\text{Cu}^+ + e \rightarrow \text{Cu}_{\text{lattice}}$. Dimensionless currents for the cases of ad-atom Cu^0 and ad-ion Cu^+ were given by Equations 29 and 32, respectively. In these cases, extra parameters, η and θ_0 , remain because of the inapplicability of the above treatment to J/J_∞ . Transients of dimensionless current J at various N_2 values and $\eta = -50$ mV calculated from

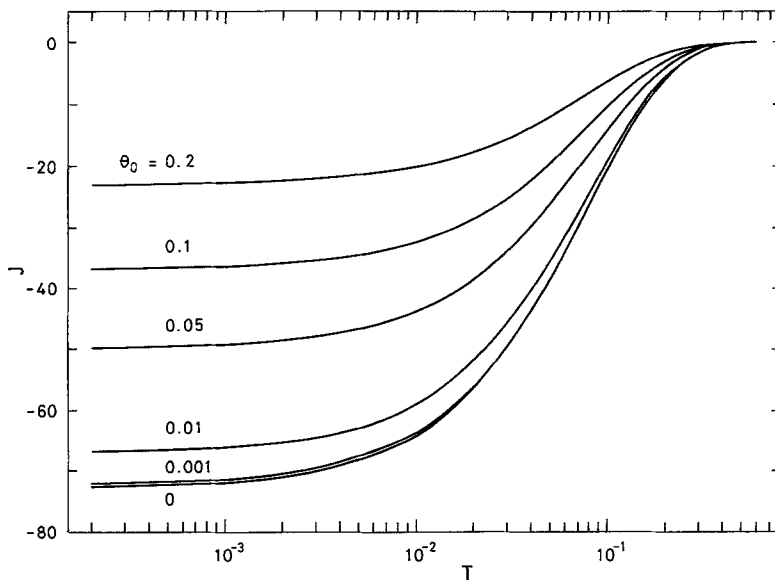


Fig. 9. The relationship between J and time with varying θ_0 at OFF in the case of ad-ion Cu^+ , $\eta = -50$ mV, $N_3 = 10$.

Equations 29 and 32 are shown in Figs. 6 and 7 for ad-atom Cu^0 and ad-ion Cu^+ , respectively. The transient behaviour resembles that for the ON mode. It is worth noting that a reduction current is observed in the case of ad-ion Cu^+ when N_2 is small. This could happen if the incorporation rate of copper into the lattice in steps, as a result of the reaction: $\text{Cu}^+ + e \rightarrow \text{Cu}_{\text{lattice}}$ exceeds the oxidation rate to cupric ions through the reaction $\text{Cu}^+ \rightarrow \text{Cu}^{2+} + e$; whereas the reduction current does not appear for ad-atom Cu^0 , since the reaction $\text{Cu}^0 \rightarrow \text{Cu}_{\text{lattice}}$ takes place and there is no charge transfer. In the former case, the oxidation reaction becomes predominant and the above phenomenon cannot be observed any more, as the N_2 value becomes large. The dependence of J -time curves on overpotential and surface coverage are shown in Figs. 8 and 9.

References

- [1] M. Fleischmann and H. R. Thirsk, *Electrochim. Acta* **2** (1960) 22.
- [2] M. Fleischmann and J. A. Harrison, *Electrochim. Acta* **11** (1966) 749.
- [3] M. Fleischmann, S. K. Rangarajan and H. R. Thirsk, *Trans. Faraday Soc.* **63** (1967) 1240.
- [4] A. Damjanovic and J. O'M. Bockris, *J. Electrochem. Soc.* **110** (1963) 1035.
- [5] J. A. Harrison, *J. Electroanal. Chem.* **18** (1968) 337.
- [6] J. O'M. Bockris and A. Damjanovic, 'Modern Aspects of Electrochemistry', Vol. 3 (edited by J. O'M. Bockris and B. E. Conway) Butterworths, London (1964) Ch. 4.
- [7] J. A. Harrison and H. R. Thirsk, 'Electroanalytical Chemistry', Vol. 5 (edited by A. J. Bird) Marcel Dekker, New York (1971) Ch. 2.
- [8] J. O'M. Bockris and H. Kita, *J. Electrochem. Soc.* **109** (1962) 928.
- [9] H. S. Carslaw and J. C. Jaeger, 'Conduction of Heat in Solids', Oxford University Press, London (1959) p. 93.
- [10] E. Mattson and J. O'M. Bockris, *Trans. Faraday Soc.* **55** (1959) 1586.
- [11] M. Fleischmann, S. K. Rangarajan and H. R. Thirsk, *Trans. Faraday Soc.* **63** (1967) 1256.